九州大学学術情報リポジトリ
Kyushu University Institutional Repository

# Autonomous System Concept of Multiple-Receiver Inductive Coupling Wireless Power Transfer for Output Power Stabilization Against Cross-Interference Among Receivers and Resonance Frequency Tolerance

Ishihara, Masataka
Graduate School of Natural Science and Technology, Okayama University

Fujiki, Keita
Graduate School of Natural Science and Technology, Okayama University

Umetani, Kazuhiro
Graduate School of Natural Science and Technology, Okayama University

Hiraki, Eiji
Graduate School of Natural Science and Technology, Okayama University

https://hdl.handle.net/2324/7449720

出版情報：IEEE Transactions on Industry Applications. 57 (4), pp.3898-3910, 2021-05-18. IEEE
バージョン：
権利関係：© 2021 IEEE. Personal use of this material is permitted. Permission from IEEE must be obtained for all other uses, in any current or future media, including reprinting/republishing this material for advertising or promotional purposes, creating new collective works, for resale or redistribution to servers or lists, or reuse of any copyrighted component of this work in other works.

KYUSHU UNIVERSITY

# Autonomous System Concept of Multiple-Receiver Inductive Coupling Wireless Power Transfer for Output Power Stabilization Against Cross-Interference Among Receivers and Resonance Frequency Tolerance

Masataka Ishihara, Keita Fujiki, Kazuhiro Umetani, Eiji Hiraki
Graduate School of Natural Science and Technology
Okayama University
Okayama, Japan

Published in: IEEE Transactions on Industry Applications
( Volume: 57, Issue: 4, July-Aug. 2021)

© 2021 IEEE. Personal use of this material is permitted. Permission from IEEE must be obtained for all other uses, in any current or future media, including reprinting/republishing this material for advertising or promotional purposes, creating new collective works, for resale or redistribution to servers or lists, or reuse of any copyrighted component of this work in other works.

DOI: 10.1109/TIA.2021.3081071

# Autonomous System Concept of Multiple-Receiver Inductive Coupling Wireless Power Transfer for Output Power Stabilization Against Cross-Interference Among Receivers and Resonance Frequency Tolerance

Masataka Ishihara, *Member, IEEE*, Keita Fujiki, *Member, IEEE*, Kazuhiro Umetani, *Member, IEEE*, and Eiji Hiraki, *Member, IEEE*

***Abstract*—Multiple-receiver resonant inductive coupling wireless power transfer (RIC-WPT) technique is emerging as a promising charging method for multiple household appliances, mobile devices, and wearable devices. However, this technique often suffers from output power fluctuation owing to the cross-interference among receivers as well as the manufacturing and aging tolerance of the resonant frequency (i.e., resonant frequency tolerance). This paper proposes an autonomous RIC-WPT system concept to solve this difficulty. The proposed concept addresses the cross-interference and resonant frequency tolerance by incorporating two functions: 1. The amplitude of the transmitter current is controlled to have a constant amplitude; 2. The phase of each receiver current is controlled to be orthogonal to that of the transmitter current by using an active reactance compensator installed in each receiver. The experiment of a two-receiver RIC-WPT system successfully verified that the two functions of the proposed system concept can stabilize the output voltage against the cross-interference and resonant frequency tolerance.**

***Index Terms*—multiple-receiver, resonant inductive coupling, wireless power transfer, cross-coupling, cross-interference, component tolerance, resonant frequency, variable capacitor, active reactance compensator**

## I. Introduction

RECENTLY the resonant inductive coupling wireless power transfer (RIC-WPT) technique has attracted significant attention owing to its comparatively high efficiency and large output power. One attractive feature of the RIC-WPT is its ability to charge multiple devices simultaneously using a single transmitter [1]–[11]. This feature is advantageous for achieving a wireless charging desk [12]–[14], which can supply electric power to multiple household appliances, mobile devices, and wearables placed anywhere on the desk, without a wired connection, as illustrated in Fig. 1.

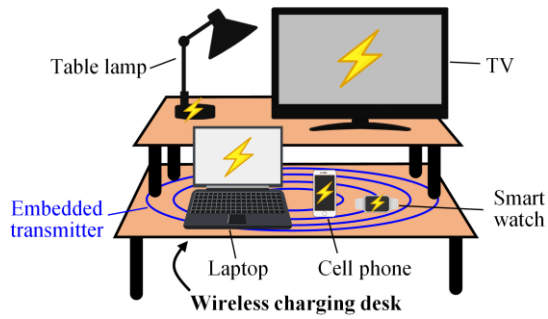


Fig. 1. Expected applications of multiple-receiver RIC-WPT technique.

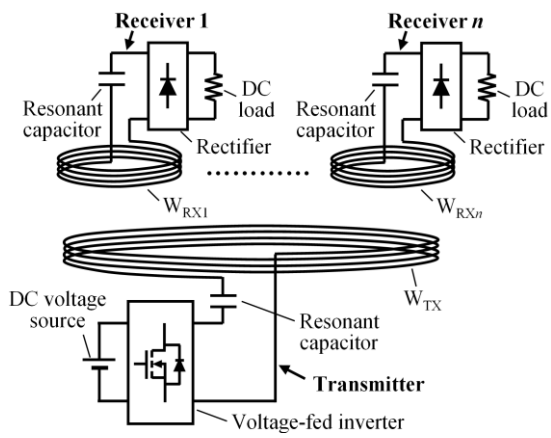


Fig. 2. Conventional multiple-receiver RIC-WPT system.

A basic RIC-WPT system for charging multiple devices comprises a transmitter and multiple receivers, as shown in Fig. 2, where $W_{TX}$ and $W_{RXk}$ ($k$ = 1, …, $n$) are the transmitter and receiver coils, respectively. In the transmitter, an AC voltage source comprising a DC voltage source and a voltage-fed inverter supplies a high-frequency AC current to the transmitter

This article was presented in part at the 2019 IEEE Energy Conversion Congress and Exposition, Baltimore, MD, USA, Sep. 29–Oct. 3 [11].
*(Corresponding author: Masataka Ishihara.)*

M. Ishihara, K. Umetani, and E. Hiraki are with the Graduate School of Natural Science and Technology, Okayama University, Okayama, Japan (e-mail: p4wv0vf6@s.okayama-u.ac.jp; umetani@okayama-u.ac.jp; hiraki@okayama-u.ac.jp).

Keita Fujiki was with the Graduate School of Natural Science and Technology, Okayama University, Okayama, Japan. He is now with the Toshiba Mitsubishi-Electric Industrial Systems Corporation, Kobe, Japan (e-mail: FUJIKI.keita@tmeic.co.jp).

resonator, thus generating an AC magnetic field; this AC magnetic field induces a voltage in the receiver coil, exciting the resonance of the receiver resonator. Finally, DC power is obtained by rectifying the resonance current. The receiver resonator is commonly designed to have the same resonant frequency as the frequency of the AC current of the transmitting coil [15] to excite a large resonance at the receiver resonator, resulting in increased efficiency and output power.

Despite the attractive features, the multiple-receiver RIC-WPT system often suffers from difficulty in stabilizing the output power of each receiver due to the following two causes. The first cause is the deviation of the resonant frequency of a receiver resonator from the frequency of the transmitter current due to manufacturing tolerances or the aging effect of the resonant capacitors and receiver coils, which is referred to as the resonant frequency tolerance in this paper. Particularly, the receiver resonator is commonly designed to have a high Q factor for achieving a high efficiency [16], [17]. In this design, the amplitude of the resonance current in the receiver resonator is sensitive to the resonant frequency tolerance, resulting in unstable output power. The second cause is the cross-interference among multiple receivers. In the multiple-receiver WPT system, the operation of one receiver can affect the output powers of other receivers directly and indirectly. In the direct effect, the coil current in one receiver induces AC voltages in the coils of the other receivers, which affects the receiver coil current and consequently the output powers of the other receivers. In the following sections, this direct effect is referred to as direct interference, which has also been referred to as cross-coupling in several previous studies [3]–[11]. In the indirect effect, the coil current of one receiver induces an AC voltage in the transmitter coil, which affects the transmitter coil current and, consequently, the output powers of the other receivers. In the following sections, this indirect effect is referred to as indirect interference. Given that the stability of the output power is an essential quality for ensuring a wide charging area, this problem should be solved for charging multiple devices shown in Fig. 1.

Conventionally, several preceding techniques [18]–[24] have addressed the resonant frequency tolerance. For example, [18], [19] proposed an active compensator for the inductance of the transmitter coil against manufacturing tolerance and the aging effect. Additionally, [20], [21] have also proposed a compensator for the receiver, based on these techniques; [22]–[24] has proposed the application of an active rectifier. Regarding the problem caused by indirect interference, [2], [4], [7]–[9] have proposed to control the transmitter current at a constant amplitude regardless of the load of each receiver operation. The transmitter current with a constant amplitude can be achieved by feedback control of the DC voltage source or voltage-fed inverter [25]. Alternatively, an LCC topology [2], [26] or a K-inverter [8], [9] may be adapted to the transmitter to achieve the transmitter current with a constant amplitude. Furthermore, to address the direct interference, [3]–[5] have proposed inserting an appropriate reactance to cancel the induced voltage due to the direct interference. However, this appropriate reactance depends on the load of each receiver and

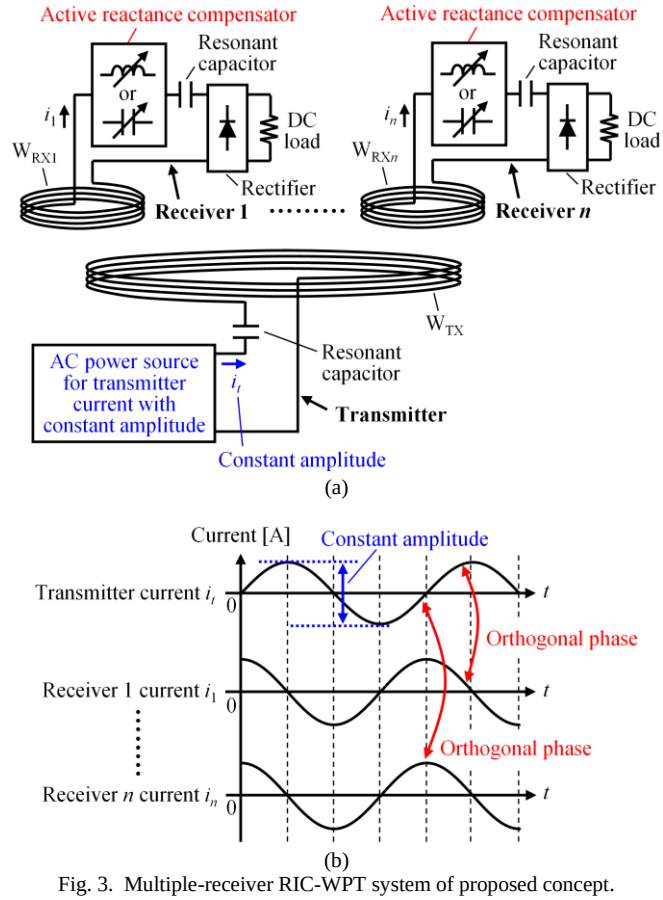


Fig. 3. Multiple-receiver RIC-WPT system of proposed concept. (a) System configuration. (b) Key waveforms.

the magnetic coupling among the receivers, and therefore this method may be practically difficult for practical RIC-WPT systems, which tend to have dynamically changing load conditions. As mentioned above, these techniques have proven to solve the problems partly. However, they still face challenges with regard to solving these problems entirely.

The purpose of this paper is to propose a novel system concept of the multiple-receiver RIC-WPT system, which can automatically solve the effect of the resonant frequency tolerance and the cross-interference (both of the direct and indirect interference) among multiple receivers. Fig. 3 shows the basic idea and key waveforms of the proposed system concept, where $i_k$ ($k = t, 1, \ldots, n$) represents the current of the corresponding coil. The proposed system concept incorporates the two functions to solve the aforementioned two causes: 1. The amplitude of the transmitter current is controlled to have a constant amplitude regardless of the presence/absence of the receivers or a load of each receiver; 2. The phase of the receiver coil current is controlled to be orthogonal to that of the transmitter coil current. The former function (hereinafter referred to as function 1) is effective in solving the indirect interference, similarly as in the preceding techniques. The latter function (hereinafter referred to as function 2) is effective in solving the resonant frequency tolerance and direct interference, as shown later in this paper. For adjusting the phase of the receiver current, we inserted an active reactance compensator in series to the receiver coil of each receiver. The specific circuit

configuration of the active reactance compensator and its control strategy are discussed in section III of this paper.

This paper is an updated version of the conference paper [11]. Based on [11], this paper further adds the experimental results of the systems with only one of the aforementioned two functions. The purpose of adding these experimental results is to elucidate that both functions are essential for stabilizing the output power of the multiple-receiver RIC-WPT system against cross-interference. Additionally, this paper includes a detailed description on a possible approach to practically implement the proposed system concept in section III, which was not discussed in [11]. Besides, this paper discusses the detailed reason why the proposed system concept is valid regardless of the number of the receiver.

The remainder of this paper is structured into four sections. Section II presents the basic idea for the proposed RIC-WPT system concept and discusses how this concept can stabilize the output power against the resonance frequency tolerance and cross-interference. Section III discusses the practical implementation approach of the proposed RIC-WPT system concept. Section IV presents the experiment that validates the output power stabilization by the proposed system concept. Finally, section V gives the conclusions.

## II. Proposed System Concept

This section first discusses the system configuration of the proposed system concept to achieve the two functions. Second, this section shows how the constant transmitter current can eliminate the output fluctuation caused by indirect interference. Third, this section shows how the receiver current phase orthogonal to the transmitter current phase can eliminate the output power fluctuation caused by direct interference and resonant frequency tolerance. For simplifying the discussion, hereafter, it is assumed that the quality factors of the resonators are high enough to adopt the first harmonic approximation analysis, as is common in many practical RIC-WPT systems [1], [15].

### A. System Configuration

The proposed system concept of Fig. 3 (a) comprises the following two parts.

The first is the transmitter with an AC power source that can adjust the amplitude of the transmitter current, as shown in Fig. 3 (a). This AC power source works to maintain the amplitude of the transmitter current regardless of each receiver operation, as shown in Fig. 3 (b), resulting in a stable magnetic field.

The second is the receiver with an active reactance compensator to adjust the phase of the receiver current, as shown in Fig. 3 (a). The compensator operates as a variable capacitor or a variable inductor that adjust small reactance that the fixed circuit parameters of the receiver resonator cannot adjust. The active reactance compensator dynamically adjusts the reactance in the receiver so that the phase of the receiver current is orthogonal to the phase of transmitter current, as shown in Fig. 3 (b).

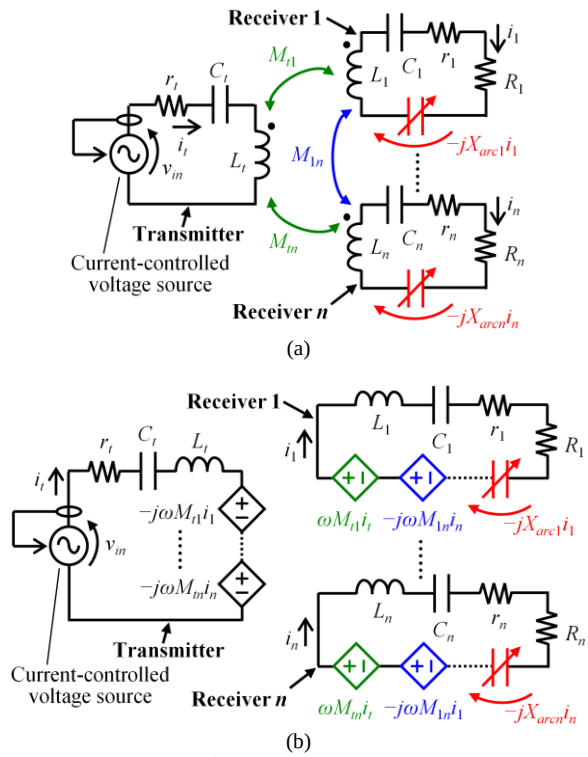


Fig. 4. Equivalent circuit of Fig. 3 (a). (a) Model based on coupling circuit. (b) Model based on induced voltage.

### B. Effect of Constant Amplitude of Transmitter Current

Fig. 4 shows the equivalent circuit of Fig. 3 (a), where the active reactance compensators are represented as the variable capacitors, and these reactances are denoted as $X_{arck}$ ($k = 1, \ldots, n$). Besides, the AC power source for the constant amplitude of the transmitter current is represented as the current-controlled voltage source, and this sinusoidal voltage is denoted as $v_{in}$. In Fig. 4, $L$, $r$, and $C$, with different subscripts ($t$, 1, …, $n$), are the self-inductances, parasitic resistances, and capacitances of the corresponding coil, respectively; $R_k$ ($k = 1, \ldots, n$) are the equivalent AC load resistances representing the power loss at the rectifier and the DC load resistance; $M_{tk}$ ($k = 1, \ldots, n$) are the mutual inductance between $W_{TX}$ and the corresponding receiver coil; $M_{kl}$ ($k, l = 1, \ldots, n$; $k \neq j$; and $M_{lk} = M_{kl}$) are the mutual inductance between the corresponding receiver coils. The magnetic couplings in Fig. 4 (a) can be replaced with the induced voltage, as shown in Fig. 4 (b). Then, according to

$$\begin{bmatrix} v_{in} \\ 0 \\ 0 \\ \vdots \\ 0 \end{bmatrix} = \begin{bmatrix} r_t + jX_t & -j\omega M_{t1} & -j\omega M_{t2} & \cdots & -j\omega M_{tn} \\ j\omega M_{t1} & -(r_1+R_1)-j(X_1+X_{arc1}) & 0 & \cdots & 0 \\ j\omega M_{t2} & 0 & -(r_2+R_2)-j(X_2+X_{arc2}) & \cdots & 0 \\ \vdots & \vdots & \vdots & \ddots & \vdots \\ j\omega M_{tn} & 0 & 0 & \cdots & -(r_n+R_n)-j(X_n+X_{arcn}) \end{bmatrix} \begin{bmatrix} i_t \\ i_1 \\ i_2 \\ \vdots \\ i_n \end{bmatrix} \quad (1)$$

Kirchhoff's voltage law, the operation of each resonator in Fig. 4 can be described as (1), where $X_t = \omega L_t - 1/\omega C_t$ and $X_k = \omega L_k - 1/\omega C_k$ ($k = 1, \ldots, n$). In (1), the magnetic coupling between any pair of receivers (i.e., direct interference) is ignored (i.e., $M_{kl} = 0$) because this subsection discusses elimination only of the indirect interference, which can be achieved by adopting the constant amplitude of the transmitter current. The method for eliminating direct interference is discussed in the next subsection. From (1), $i_t$ and the output power of each receiver $P_k$ ($k = 1, \ldots, n$) can be obtained, respectively, as

$$i_t = v_{in} \Big/ \left[ r_t + jX_t + \sum_{k=1}^{n} \frac{\omega^2 M_{tk}^{\ 2}}{(r_k + R_k) + j(X_k + X_{arck})} \right], \tag{2}$$

$$P_k = R_k |i_k|^2 = R_k \left| \frac{j\omega M_{tk} i_t}{(r_k + R_k) + j(X_k + X_{arck})} \right|^2. \tag{3}$$

From (2), if $v_{in}$ is fixed, $i_t$ depends on the circuit parameters of the transmitter and all receivers. Therefore, in the conventional system of Fig. 2, from (3), the output power of each receiver is affected by other receivers because $v_{in}$ is fixed. To solve this problem, we must adjust $i_t$ to be constant. In other words, the constant amplitude of the transmitter current can eliminate the output power fluctuation due to indirect interference.

Notably, the output power of each receiver can be controlled independently, even under the condition of constant transmitter current amplitude. In the proposed system concept, the output power of each receiver can be controlled by adjusting $R_k$ in (3). Therefore, each receiver in the proposed system concept is assumed to have an active rectifier [22]–[24] or DC-DC [27] converter for adjusting the value of $R_k$. Certainly, fixing the transmitter current at a constant amplitude may reduce the efficiency when the output power of the receivers is small. However, in relatively low power applications, such as the wireless charging desk, the reduction of the efficiency does not lead to large power loss, and therefore the constant amplitude of the transmitter current is possibly acceptable.

### *C. Effect of Receiver Current Phase Orthogonal to Transmitter Current Phase*

Fig. 5 shows the phasor diagrams when $X_{arck}$ are adjusted so that the phase of each receiver current is orthogonal to the phase of the transmitter current, where $I$, with different subscripts [$t$ and $k$ ($k = 1, \ldots, n$)], denotes the effective values of the corresponding current, and the phase angle of $i_t$ is defined as $-\pi/2$ as a reference. In the following discussion, the direct interference is considered (i.e., $M_{kl} \neq 0$). As shown in Fig. 5, the phases of the voltage drop caused by the resonant frequency tolerance (i.e., $X_k i_k$) are always orthogonal to the phase of $i_k$,

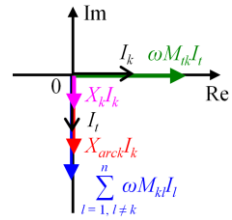


Fig. 5. Phasor diagram of receiver $k$ ($k = 1, \ldots, n$) in Fig. 4

because $X_k$ represent pure reactances. Furthermore, the phases of the voltages induced by direct interference (i.e., the phasors in blue) are always orthogonal to the phases of $i_k$ because the phases of all receiver current are orthogonal to the phase of $i_t$.

Based on Kirchhoff's voltage law and Fig. 5, the operation of the receivers in Fig. 4 can be described as (4). By extracting the real parts of (4) and solving for $I_k$, each receiver current can be derived as

$$I_k = \omega M_{tk} I_t \big/ (r_k + R_k). \tag{5}$$

From (5), it can be seen that each receiver current is unaffected by the circuit parameters of the other receivers. Thereafter, by extracting the imaginary parts of (4) and substituting (5) for $I_k$, $X_{arck}$ can be obtained as

$$X_{arck} = -X_k - \sum_{l=1, l\neq k}^{n} \frac{\omega M_{kl} M_{tl} (r_k + R_k)}{M_{tk} (r_l + R_l)}. \tag{6}$$

In this case, the imaginary parts of (4) are zero, which implies that the voltages of $X_{arck}$ operate to entirely cancel the voltages induced by the direct interference and resonant frequency tolerance. Finally, from (5), we can obtain the output powers of the receivers as

$$P_k = R_k I_k^{\ 2} = R_k \left[ \omega M_{tk} I_t \big/ (r_k + R_k) \right]^2, \tag{7}$$

From (7), it can be seen that the output power of each receiver is unaffected by the direct interference, as well as the resonant frequency tolerance, under the constant transmitter current amplitude.

Certainly, [3]–[5] have already elucidated that direct interference can be eliminated by inserting the reactance to each receiver appropriately, although the resonant frequency tolerance has not been considered. In fact, (6) with $X_k = 0$ and equation (29) in [4] are the same. However, the strategy for inserting the reactance to each receiver appropriately differs between this study and previous studies of [3]–[5]. The previous studies suggest that the estimation of the mutual inductances among receiver coils and the output and parasitic resistances of all receivers are necessary to insert the reactances appropriately. This is because (6) with $X_k = 0$ depends on the

$$\begin{bmatrix} 0 \\ 0 \\ \vdots \\ 0 \end{bmatrix} = \begin{bmatrix} j\omega M_{t1} & (r_1 + R_1) + j(X_1 + X_{arc1}) & j\omega M_{12} & \cdots & j\omega M_{1n} \\ j\omega M_{t2} & j\omega M_{12} & (r_2 + R_2) + j(X_2 + X_{arc2}) & \cdots & j\omega M_{2n} \\ \vdots & \vdots & \vdots & \ddots & \vdots \\ j\omega M_{tn} & j\omega M_{1n} & j\omega M_{2n} & \cdots & (r_n + R_n) + j(X_n + X_{arcn}) \end{bmatrix} \begin{bmatrix} jI_t \\ I_1 \\ I_2 \\ \vdots \\ I_n \end{bmatrix} \tag{4}$$

mutual inductances among receiver coils and the output and parasitic resistances of all receivers. Usually, the real-time estimations of these circuit parameters and real-time calculation of the reactance are very complicated. Therefore, although the theoretical framework has been established, a practical method for inserting the reactance to each receiver appropriately to compensate for direct interference has not been elucidated yet. However, as shown in this subsection, we can eliminate direct interference without the need for complicated parameter estimations and calculations by inserting the reactance based on the phase relation between the receiver and transmitter currents, although the phase of the transmitter current must be sensed. Besides, the inserting strategy based on the phase relationship can eliminate the influence caused by the resonant frequency tolerance simultaneously.

Another attractive feature of the proposed system concept is that the direct interference can be eliminated with a fixed single operating frequency. To eliminate the effect of the direct interference, [1] and [6] have proposed to transfer the power with multiple operating frequencies. According to their approach, the transmitter generates an AC magnetic field at multiple frequencies, and each receiver selectively receives the electric power at a frequency assigned to the receiver by utilizing a band-pass filter. Therefore, this approach requires the tuning of the band-pass filter at different operating frequencies, which may complicate the receiver circuit design. Furthermore, this approach is difficult to apply under the severely limited allowable operating frequency bandwidth, which tends to be required in the industrial application of RIC-WPT systems [27].

## III. Practical Implementation of Proposed System Concept

In this section, we show the practical implementation approach of the proposed system concept, which achieves the two functions. The first subsection discusses the overall system structure and also describes a technical issue relating to the practical implementation of the proposed system concept. Furthermore, the second subsection discusses a practical circuit configuration and the control strategy for the active reactance compensator.

### A. Overall System Structure

Fig. 6 shows the practical implementation approach of the proposed system concept given in Fig. 3. As in Fig. 3, Fig. 6(a) comprises the following two parts.

The first is the transmitter that senses the amplitude of the transmitter current and controls. As shown in Fig. 6(a), this paper adopts the control of the variable DC voltage source of the voltage-fed inverter for achieving the transmitter current with a constant amplitude. However, the method to achieve the transmitter current with a constant amplitude is not especially limited. The sensing circuit obtains the amplitude of the transmitter current, and the controller on the transmitter side controls the variable DC voltage source so that the amplitude of the transmitter current is kept constant. In an actual system, the variable DC voltage source can be achieved by feedback control

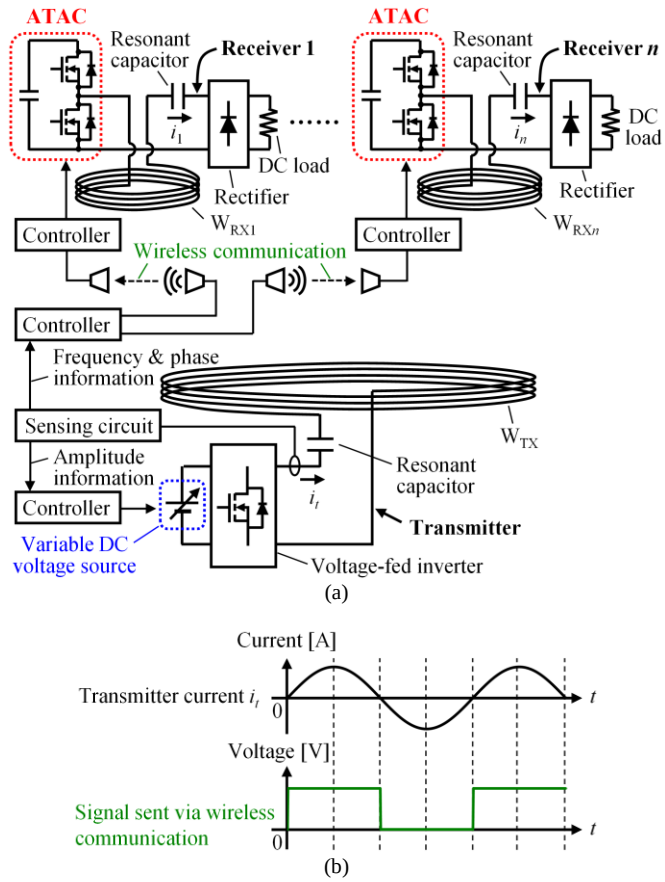


Fig. 6. Practical implementation approach of Fig. 3 (a). (a) System configuration. (b) Example of signal sent via wireless communication.

of a DC-DC converter.

The second is the receiver with a simple switching circuit, referred to as an automatic tuning assist circuit (ATAC) [18], [28], [29] and its controller as the active reactance compensator, which operates based on the information of the phase and frequency of the transmitter current. The phase and frequency information of the transmitter current is transmitted to the receiver controller via the wireless communication. Then, the controller of the receiver generates the gating signals for the semiconductor power switches of the ATAC, based on the phase and frequency information. As discussed in the next subsection, the gating signals of the ATAC has the same frequency as the transmitter coil current, a fixed duty ratio of 50%, and a constant phase difference to the transmitter coil current. Therefore, if the phase and frequency of the transmitter coil current are supplied via wireless communication, the receiver controller does not need to sense the circuit parameters. The simplest method to transmit this information may be to broadcast the real-time polarity of the transmitter coil current in a binary code, as shown in Fig. 6 (b), because the phase and frequency of the broadcasted signal are equal to those of the transmitter coil current. Then, the gating signals for the ATAC can be generated by just shifting the phase of the received signals of the real-time polarity of the transmitter coil by a constant phase angle.

However, a practical implementation of the wireless

communication method is beyond the scope of this paper because an appropriate method for wireless communication has not been elucidated yet. In other words, the wireless communication method remains a technical issue for the practical implementation of the proposed system concept. In this sense, this paper remains to propose a system concept for the multiple-receiver RIC-WPT system. However, in the future, there is a possibility of establishing a wireless communication method for the proposed system concept. This is attributed to the fact that techniques for sensing the current phase of a physically separated resonator have been widely studied for various applications such as an active impedance tuning method for a repeater [28], bi-directional WPT systems [30], and active rectifiers for the RIC-WPT systems [22]. These techniques may be applied to the proposed system concept in the future. The full practical implementation of the proposed system concept, including wireless communication, will be studied in a future paper.

### *B. Active Reactance Compensator*

Recently several techniques have been proposed to configure an active reactance compensator, such as a capacitor matrix [19], [31], DC-voltage-controlled variable capacitor [32], gate-controlled series capacitor [33], mechanical variable capacitor controlled by a stepping motor [34], variable inductor [21], [35], ATAC [18], [28], [29] and self-adaptive auxiliary circuit [20] (this is the same circuit as the ATAC). Among these techniques, the ATAC may be more attractive than the other techniques to achieve function 2. The ATAC can automatically control the phase of the receiver current to match the desired phase without sensing the receiver current. Hence, this paper adopts the ATAC for each receiver to achieve function 2.

The ATAC was initially proposed in [18] for the transmitter of a single-receiver system. The preceding study of [18] proposed the ATAC to solve a problem wherein the resonant frequency tolerance caused the deviation of the resonant frequency of the transmitter from the operating frequency. This deviation is a critical issue for the RIC-WPT system because it decreases the power factor of the voltage-fed inverter, which results in lower output power and efficiency. The preceding study of [18] revealed that the transmitter with the ATAC automatically achieves a unity power factor for the voltage-fed inverter without sensing the transmitter current even if there is a deviation of the resonant frequency of the transmitter from the operating frequency. This result means that the transmitter with the ATAC can compensate for the influence of the resonant frequency tolerance. Based on [18], this paper reveals that the receiver with the ATAC operating with a control strategy, revealed in this paper, can automatically eliminate the output power fluctuation caused by not only the resonant frequency tolerance but also the direct interference simultaneously.

Fig. 7 shows the equivalent circuit of Fig. 6(a), where $v_{Ak}$ ($k$ = 1, …, $n$) are the output voltages of the ATACs. The ATAC comprises the half-bridge circuit. The full-bridge circuit is also available instead of the half-bridge circuit [29]. The DC bus of the half-bridge circuit comprises only the smoothing capacitor, where $V_{Ak_dc}$ ($k$ = 1, …, $n$) are the DC voltages of the smoothing

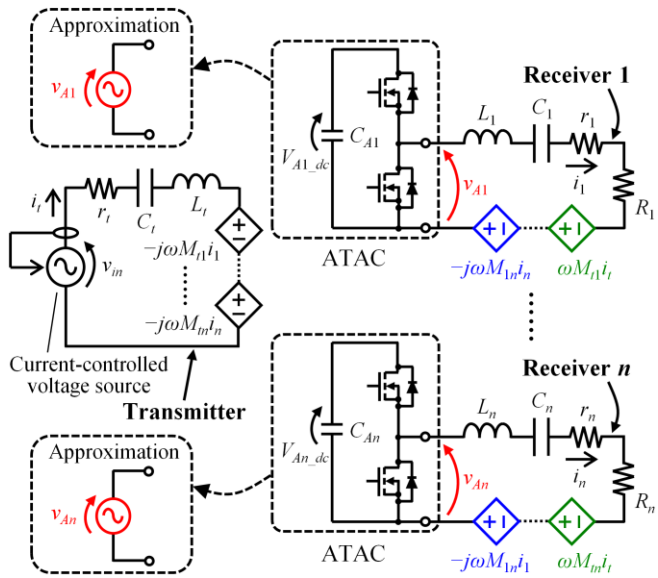

Fig. 7. Equivalent circuit of Fig. 6 (a).

capacitors, and $C_{Ak}$ ($k$ = 1, …, $n$) are the capacitances of the smoothing capacitors, which are sufficiently larger than $C_k$. Note that the DC bus of the half-bridge circuit does not have any additional DC voltage source. The ATAC automatically generates a DC voltage in the smoothing capacitor by using the resonator current. The half-bridge circuit of the ATAC operates at the same switching frequency as the transmitter current at a duty cycle of 50%. Besides, the half-bridge circuit of the ATAC operates with a fixed phase difference from the transmitter current and applies a rectangular wave voltage from the intermediate point of the half-bridge circuit to the receiver. Based on this operation, in the equivalent circuit, the ATAC can be described as the AC voltage source.

Ideally, the ATAC does not have any resistive components because the ATAC consists only of the half-bridge circuit and the smoothing capacitor. Therefore, the ATAC does not receive effective power in the steady-state and operates as a reactive component. In other words, in the steady-state, the phase of the output voltage of the ATAC must be orthogonal to that of the resonator current (i.e., current outputted from the intermediate point of the half-bridge circuit of the ATAC). Hence, the ATAC behaves to inject a reactance into a resonator so that the phase of the resonator current is orthogonal to the phase of the output voltage of the ATAC by adjusting the smoothing capacitor voltage automatically. Therefore, the ATAC can be interpreted as a circuit in which the phase of the resonator current can be freely adjusted according to the output voltage phase of the ATAC.

To achieve the phase relationship shown in Fig. 3 (b), the half-bridge circuit of each ATAC only needs to operate so that the phase difference between the output voltage of the ATAC and $i_t$ is $\pi$. Because the half-bridge circuit of each ATAC operates based on the information of the transmitter current, the ATAC is not required to sense the phase of the receiver currents. Fig. 8 shows the phasor diagram in this condition, where the phase angle of $i_t$ is defined as $-\pi/2$ as a reference, and $V_{Ak}$ denote the effective values of $v_{Ak}$. Fig. 9 shows the key waveforms of

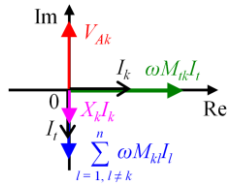


Fig. 8. Phasor diagram of receiver $k$ ($k$ = 1, …, $n$) in Fig. 7.

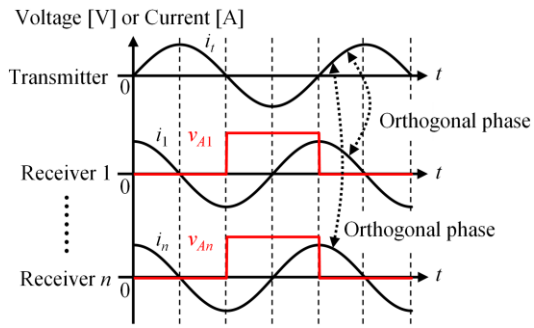


Fig. 9. Key waveforms of Fig. 7 in zero-voltage-switching (ZVS) operation.

Fig. 7 in the steady-state. Based on the operating principle of the ATAC, the phases of $i_k$ are orthogonal to the phases of $v_{Ak}$. As a result, the phase of each receiver current is orthogonal to the phase of the transmitter current. The ATAC operates to cancel the unwanted voltages caused by the direct interference and resonant frequency tolerance. Consequently, as discussed in Fig. 5, the output powers of the receivers are the same as in (7), which indicates that the output powers are unaffected by the direct interference and resonant frequency tolerance.

Next, we derive the voltage of the smoothing capacitor of the ATAC. The derived smoothing capacitor voltage is usable for the design of the voltage stress of the ATAC. First, based on the first harmonic approximation, the relationship between $V_{Ak_dc}$ and $V_{Ak}$ can be expressed as

$$V_{Ak_dc} = \frac{\pi}{\sqrt{2}} V_{Ak}. \tag{8}$$

Then, based on Kirchhoff's voltage law and Fig. 8, the operation of the receivers of Fig. 7 can be described as (9). From (8) and (9), the voltages of the smoothing capacitors of the ATAC be obtained as

$$V_{Ak_dc} = \frac{\pi}{\sqrt{2}} \frac{\omega M_{tk} I_t}{r_k + R_k} X_k + \frac{\pi}{\sqrt{2}} \sum_{l=1, l\neq k}^{n} \frac{\omega^2 M_{tk} M_{kl} I_t}{r_l + R_l}. \tag{10}$$

The first term on the right-hand side of (10) is the voltage for compensating the effect of the resonant frequency tolerance. The second term on the right-hand side of (10) is the voltage for compensating the effect of direct interference.

The smoothing capacitor of the ATAC cannot be charged with negative voltages owing to the body diodes of the half-bridge circuit. Therefore, when $V_{Ak_dc}$ of (10) fall below zero, the ATAC operates as the shorted circuit because the output voltage of the ATAC is zero. Hence, if $V_{Ak_dc}$ in (10) fall below zero, to obtain the positive voltage in the smoothing capacitor of the ATAC, the ATAC must operate so that the phase of the output voltage of the ATAC is identical to the phase of the transmitter current as shown in Fig. 10. However, in this case, the relations between $v_{Ak}$ and $i_k$ are capacitive. In the operation of Fig. 10, although the effect due to direct interference and resonant frequency tolerance can be eliminated, the half-bridge circuit of the ATAC cannot avoid the hard-switching operation. Therefore, in this case, we should rather design $X_k$ in advance so that $V_{Ak_dc}$ in (10) remain positive under possible variations of the mutual inductance.

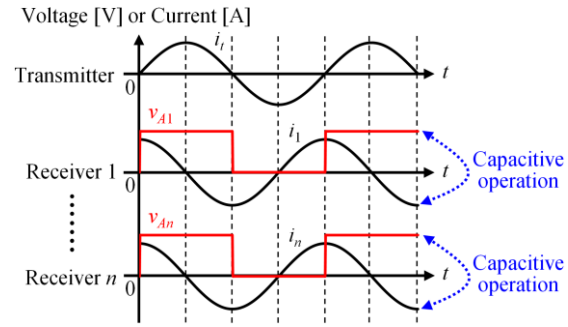


Fig. 10. Waveforms of Fig. 7 in hard switching operation.

## IV. Experiments

In this section, we carry out experiments to test the appropriateness of the proposed system concept for eliminating the output power fluctuation caused by the cross-interference and resonant frequency tolerance. In the experiments, this paper adopts a two-receiver RIC-WPT system as a representative example of the multiple-receiver RIC-WPT system (i.e., the number of receivers $n$ = 2).

### A. Experimental Setup and Conditions

Figs. 11 and 12 show the schematic and photograph of the experimental setup of the RIC-WPT system of the proposed concept, respectively, where $R_{dc1}$ and $R_{dc2}$ are the DC load resistances, and $V_{in_dc}$ is the voltage of the input DC voltage source. Table I shows the circuit parameters for the experiments, where $k_{t1} = M_{t1}/(L_t L_1)^{1/2}$. The operating frequency was set to 159.67 kHz, which was the resonant frequency of the transmitting resonator naturally implemented as a result of fabricating the transmitting resonator, although the proposed system concept does not have any limitations regarding the operating frequency. The inductance and capacitance of each receiver in Table I was determined to satisfy $X_1 \approx 0$ and $X_2 \approx 0$.

As shown in Figs. 11 and 12, the coils were arranged in the

$$\begin{bmatrix} jV_{A1} \\ jV_{A2} \\ \vdots \\ jV_{An} \end{bmatrix} = \begin{bmatrix} j\omega M_{t1} & (r_1 + R_1) + jX_1 & j\omega M_{12} & \cdots & j\omega M_{1n} \\ j\omega M_{t2} & j\omega M_{12} & (r_2 + R_2) + jX_2 & \cdots & j\omega M_{2n} \\ \vdots & \vdots & \vdots & \ddots & \vdots \\ j\omega M_{tn} & j\omega M_{1n} & j\omega M_{2n} & \cdots & (r_n + R_n) + jX_n \end{bmatrix} \begin{bmatrix} jI_t \\ I_1 \\ I_2 \\ \vdots \\ I_n \end{bmatrix} \tag{9}$$

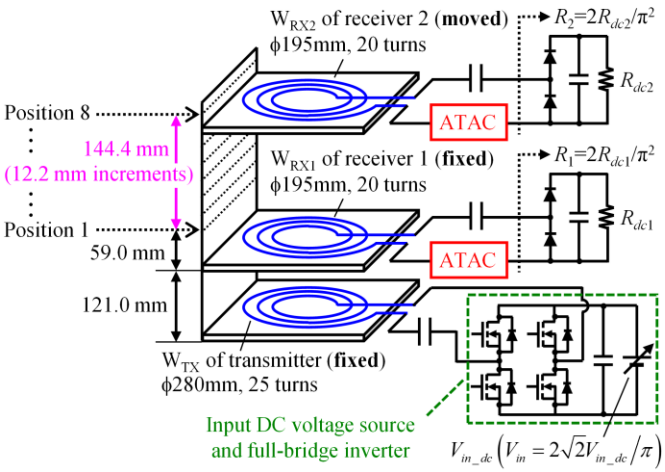


Fig. 11. Schematic of experimental setup.

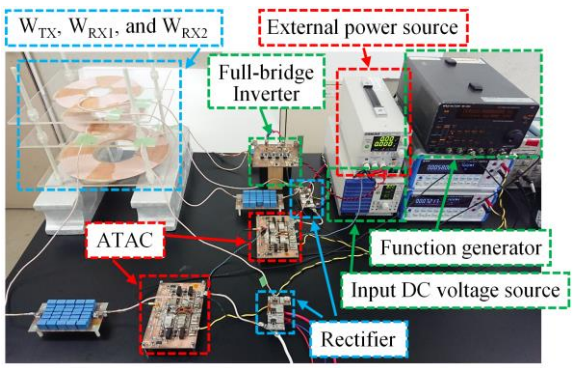


Fig. 12. Photograph of experimental setup.

vertical direction so that cross-interference strongly occurred. As a result, the appropriateness of the proposed system concept against cross-interference could be verified clearly. The coils were arranged so that the polarities of all mutual inductances were positive. In the experimental setup, the positions of $W_{TX}$ of the transmitter and $W_{RX1}$ of receiver 1 were fixed. Hence, $M_{t1}$ had a constant value. To evaluate the characteristics of the dependence on cross-interference, $W_{RX2}$ of receiver 2 was moved through eight different vertical positions, as shown in Fig. 11. Hence, $M_{t2}$ and $M_{12}$ differed depending on the position of $W_{RX2}$, respectively. Fig. 13 shows the coupling coefficients at each position of $W_{RX2}$, where, $k_{t2} = M_{t2}/(L_tL_2)^{1/2}$ and $k_{12} = M_{12}/(L_1L_2)^{1/2}$.

This section compares the characteristics of the following Systems A to D to verify that both functions are essential for eliminating the influence of cross-interference. System A is the single-receiver RIC-WPT system with only function 1. When System A was tested, an unmeasured side of the receiver was opened, which emulated the condition of the absence of another receiver. Therefore, if a multiple-receiver RIC-WPT system without the influence of cross-interference can be achieved, its experimental results should be identical to the experimental results of System A. Next, System B is the multiple-receiver RIC-WPT system that adopts the proposed system concept (i.e., the multiple-receiver RIC-WPT system with both functions). Furthermore, System C is the multiple-receiver RIC-WPT system with only function 1. Finally, System D is the multiple-receiver RIC-WPT system with only function 2. The transmitter

TABLE I
CIRCUIT PARAMETERS FOR EXPERIMENTS

| Symbols / Parameters | | Values |
|---|---|---|
| $L_t$ | Self-inductance of $W_{TX}$ | 140.52 μH |
| $L_1$ | Self-inductance of $W_{RX1}$ | 55.31 μH |
| $L_2$ | Self-inductance of $W_{RX2}$ | 55.27 μH |
| $r_t$ | Parasitic resistance of transmitter | 0.24 Ω |
| $r_1$ | Parasitic resistance of receiver 1 | 0.12 Ω |
| $r_2$ | Parasitic resistance of receiver 2 | 0.12 Ω |
| $C_t$ | Capacitance of transmitter | 7.01 nF |
| $C_1$ | Capacitance of receiver 1 | 17.92 nF |
| $C_2$ | Capacitance of receiver 2 | 17.96 nF |
| $C_{A1}$ | Capacitance of ATAC on receiver 1 | 22 μF |
| $C_{A2}$ | Capacitance of ATAC on receiver 2 | 22 μF |
| $k_{t1}$ | Coupling coefficient between $W_{TX}$ and $W_{RX1}$ | 0.101 |
| $f_s$ | Operating frequency | 159.67 kHz |
| $R_1$ | Equivalent AC load resistance of receiver 1 | 4.43 Ω |
| $R_2$ | Equivalent AC load resistance of receiver 2 | 2.05 Ω |
| $I_t$ | Transmitter current of Systems A, B, and C | 1.00 A |
| $V_{in_dc}$ | Input DC voltage of System D | 23.05 V |

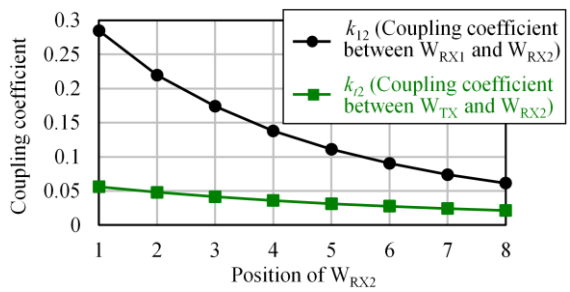


Fig. 13. Coupling coefficients between $W_{RX2}$ and other coils.

current of Systems A, B, and C was set to 1.00 A, as shown in Table I. By contrast, the input DC voltage of System D was fixed at 23.05 V. This is the input DC voltage required for System B to satisfy $I_t = 1.00$ A at Position 8, where the influence of cross-interference is minimal. In Systems A and C, the output terminals of the ATACs were shorted to emulate the condition without ATACs. Therefore, the ATAC was installed in each receiver of only Systems B and D. The comparison between the results of Systems A and B reveals that System B can eliminate the influence of cross-interference. The comparison between the results of Systems A and C reveals that the influence of cross-interference cannot be eliminated using only function 1. Similarly, the comparison between the results of Systems A and D reveals that the influence of cross-interference cannot be eliminated using only function 2.

In the experiments, the functions of the proposed system concept were conducted partially by means of manual operation. Note that the focus of this paper is not on the full practical implementation of the proposed system concept, but instead on the validation of the appropriateness of the proposed system concept. To achieve the transmitter current of a constant amplitude, the input DC voltage source was controlled manually based on the waveforms measured by an oscilloscope. Furthermore, as shown in Fig. 12, the phase difference between the output voltage of each ATAC and the transmitter current

was controlled to be π manually, using the function generator, which supplied the gating signals for the ATACs and the full-bridge inverter of the transmitter. The DC power for the gate drive circuits of the ATACs and full-bridge inverter was supplied by using a common external power source, as shown in Fig. 12.

### *B. Operating Waveforms*

Before the validation of the effectiveness of the proposed system concept, we measure the operating waveforms in the steady-state. The purpose of this exercise is to verify whether only System B achieves the two functions. In the experiment described in this subsection, $W_{RX2}$ was set at position 3, and Systems B–D were tested.

Fig. 14 shows the operating waveforms of the RIC-WPT system that adopts the proposed concept (i.e., System B). The ATAC operates so that the phase difference between the output voltage of the ATAC and transmitter current is π. Although the waveform of $v_{A2}$ is omitted in Fig. 14, $v_{A2}$ is in phase with $v_{A1}$. As a result, the phase of each receiver current is orthogonal to the phase of the transmitter current. Besides, the transmitter current achieves a value of 1.00 A.

Fig. 15 shows the operating waveforms of the RIC-WPT with only function 1 (i.e., System C). Although the transmitter current achieves a value of 1.00 A, the phase of each receiver current is not orthogonal to the phase of the transmitter current. Therefore, based on the discussion of Section II, although the effect of indirect interference can be eliminated, the effect of direct interference cannot be eliminated.

Fig. 16 shows the operating waveforms of the RIC-WPT with only function 2 (i.e., System D). The phase of each receiver current is controlled by means of the ATAC. However, the transmitter current cannot achieve a value of 1.00 A, in contrast to Systems B and C. Therefore, based on the discussion of Section II, although the effect of the direct interference can be eliminated, the effect of the indirect interference cannot be eliminated. The transmitter current decreases to 0.86 A from 1.00 A because the indirect interference is more substantial at position 3 than at position 8.

From Figs. 14–16, we can verify that only System B has two functions.

### *C. Output Power Stability Against Cross-Interference*

The primary purpose of this subsection is to validate the appropriateness of the proposed system concept against cross-interference. To achieve this purpose, we compare the dependence of the output power of each receiver in Systems A–D on the position of $W_{RX2}$. Besides, in this subsection, we validate whether the smoothing capacitor voltage in the ATAC can be modeled by (10), by comparing the calculation results of (10) and experimental smoothing capacitor voltages. Furthermore, we validate whether efficiency degradation due to the ATACs insertion can be a significant problem by comparing the efficiencies between Systems A and B.

Fig. 17 shows the output power of each receiver of Systems A–D at each position of $W_{RX2}$. As shown in Fig. 17 (a), the output power of receiver 1 in System B is almost constant

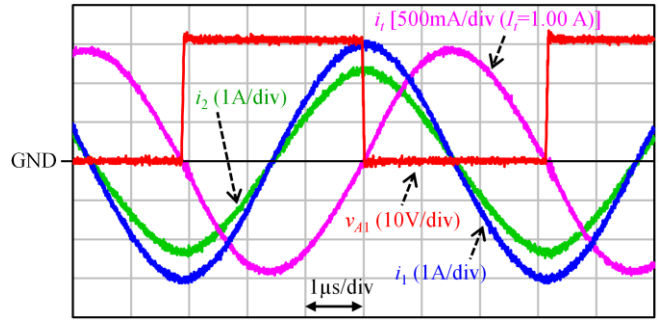


Fig. 14. Experimental waveforms of multiple-receiver RIC-WPT system of proposed concept (i.e., System B) at position 3.

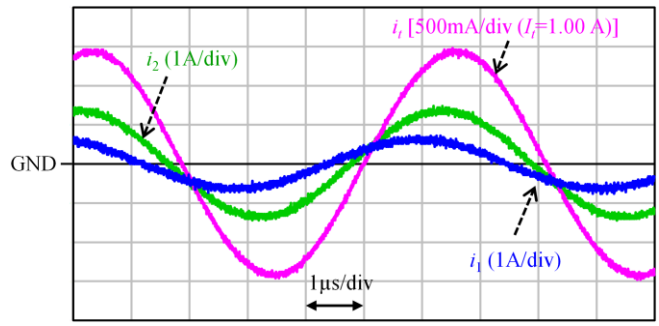


Fig. 15. Experimental waveforms of multiple-receiver RIC-WPT system with only function 1 (i.e., System C) at position 3 (The waveform of $V_{A1}$ is not shown here as the output terminals of the ATACs were shorted.).

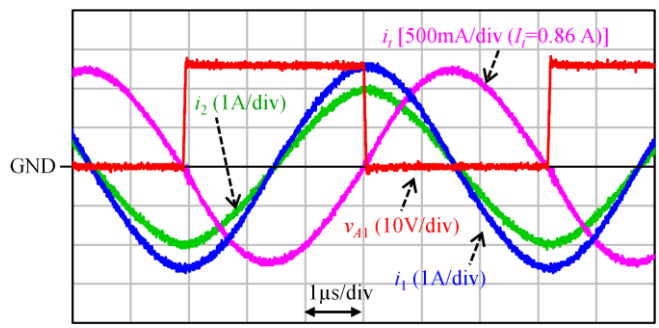


Fig. 16. Experimental waveforms of multiple-receiver RIC-WPT system with only function 2 (i.e., System D) at position 3.

regardless of the position of $W_{RX2}$. This result agrees well with the experimental result of the output power of receiver 1 in System A. Furthermore, the output power of receiver 2 in System B is also almost the same as that of System A, as shown in Fig. 17 (b). By contrast, the output power of receiver 1 in System C significantly decreases as $W_{RX2}$ approaches $W_{RX1}$. Moreover, the dependence of the output power of receiver 2 in System C on the position of $W_{RX2}$ differs considerably from that in System A. The reason why the experimental results of System C differs significantly from those of System A can be interpreted as that the voltage induced in the receivers due to the direct interference significantly affected the receiver coil current. Certainly, at positions 5–8, the output power of receiver 2 in System C is larger than those in System B because receiver 1 operates as a repeater [28], [29] to relay the magnetic field from $W_{TX}$ to $W_{RX2}$ [6]. Nevertheless, System C may not be practical because direct interference strongly affects the output power of each receiver. Then, the output power of each receiver in System D deviates from that of System A as $W_{RX2}$

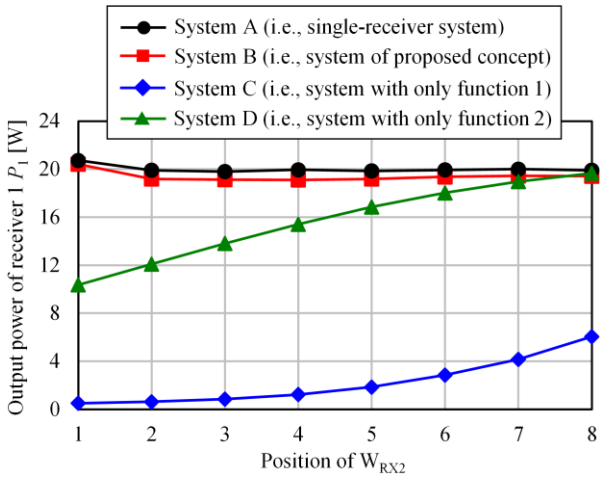


(a)

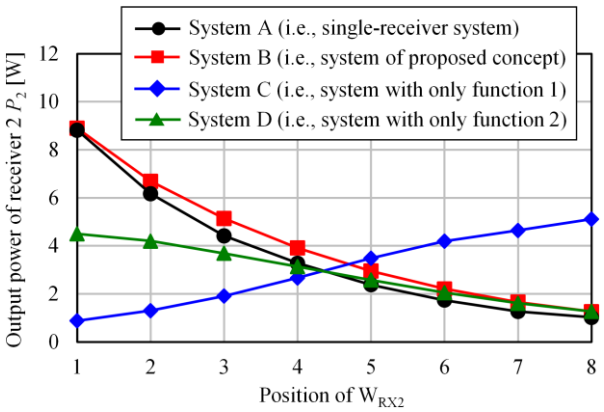


(b)

Fig. 17. Experimental results of output power at each position of $W_{RX2}$. (a) Receiver 1. (b) Receiver 2.

approaches $W_{TX}$ and $W_{RX1}$. The reason of this deviation can be interpreted as that the transmitter current is reduced as $W_{RX2}$ approaches $W_{TX}$ due to the indirect interference. As a result, the output power of each receiver in System D decreased compared with that of System A. Consequently, the appropriateness of the proposed system concept against cross-interference was validated.

Furthermore, Fig. 18 shows the smoothing capacitor voltages of the ATACs in System B at each position of $W_{RX2}$. The smoothing capacitor voltages of the ATACs increase as $W_{RX2}$ approaches $W_{RX1}$ because the induced voltage due to direct interference, to be compensated by the ATAC, increases. The experimental results are in relatively good agreement with the theoretically calculated results. Therefore, the appropriateness of (10) was validated.

Next, Fig.19 shows the comparison of the efficiency between System A and System B. The measurement of the efficiency considered the power loss of the full-bridge inverter and rectifier. The input and output powers for calculating the efficiency of System A were defined as the sum of the powers measured separately for each receiver. From, Figs. 19 and 18, the efficiency degradation due to the ATACs insertion tends to be large as the smoothing capacitor voltages of the ATACs increase. Hence, the additional power loss by inserting the ATACs is assumed to be mainly caused by the switching loss

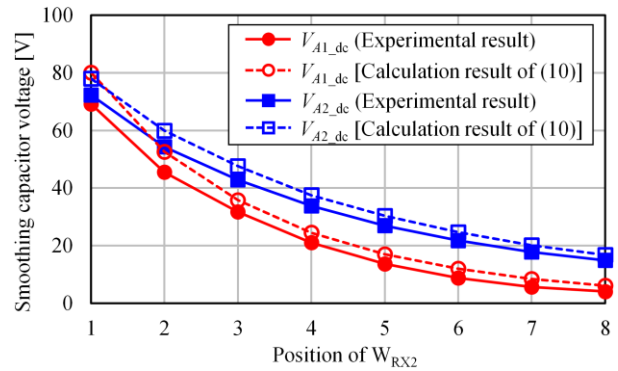


Fig. 18. Experimental and calculation results of smoothing capacitor voltages of ATACs in System B at each position of $W_{RX2}$.

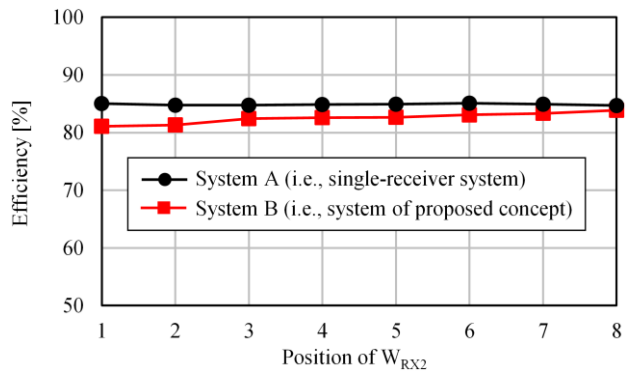


Fig. 19. Experimental efficiencies in Systems A and B at each position of $W_{RX2}$.

of the ATACs. However, owing to the zero-voltage switching operations of the ATACs, the efficiency degradation caused by inserting the ATACs is relatively low. Therefore, in most cases, efficiency degradation by inserting the ATACs may not be a serious problem.

### *D. Output Power Stability Against Resonant Frequency Tolerance*

The purpose of this subsection is to validate that the proposed system concept eliminates the output power fluctuation due to the resonant frequency tolerance of the receiver resonator. To achieve this purpose, the experimental output powers of the receivers in Systems A and B are evaluated under the condition that $C_1$ changes by ±10% from the nominal value, satisfying $X_1 = 0$. In these experiments, receiver 2 was fixed to position 3. The other circuit parameters were the same as the values provided in Table I.

Fig. 20 shows the experimental results of the output powers against the variation in $C_1$. As shown in Fig. 20, the output power of receiver 1 in System A decreases as the deviation of $C_1$ from the nominal value increases. By contrast, the output power of receiver 1 in System B is almost constant regardless of the variation in $C_1$, owing to the operation of the ATAC. Besides, the output power of receiver 2 in System B does not depend on the variation in $C_1$ because the current in receiver 1 is constant owing to the ATAC on receiver 1. From the above results, the effectiveness of the proposed system concept against the resonant frequency tolerance was validated.

## V. Conclusion

Each receiver in the multiple-receiver RIC-WPT system often suffers from output power fluctuation owing to the resonant frequency tolerance and cross-interference, which can be classified as direct and indirect interferences. To solve this problem, this paper proposed the autonomous RIC-WPT system concept that can stabilize the output power against cross-interference and resonant frequency tolerance. The proposed system concept has two functions. First, to solve the problem caused by indirect interference, the amplitude of the transmitter current is adjusted to be constant regardless of the presence/absence of the receivers or a load of each receiver. Second, to solve the problem caused by direct interference and resonant frequency tolerance, the phase of the receiver current is adjusted to be orthogonal to the phase of the transmitter current using an active reactance compensator, which operates based on the information of the phase and frequency of the transmitter current. In this study, the ATAC was adopted as the active reactance compensator owing to its simple control. We conducted experiments to validate the appropriateness of the proposed system concept. The experimental results show that the proposed system concept can stabilize the output power regardless of the cross-interference and resonant frequency tolerance.

Certainly, the part tested in this paper of the proposed system concept has a limitation that the information of the phase and frequency of the transmitter current is sent to each receiver by wired communication. However, in the future, a wireless communication method for the proposed system concept might be developed, making the proposed system concept a promising candidate as a practical method for achieving a stable multiple-receiver RIC-WPT system that is robust against cross-interference and resonant frequency tolerance.

## References


[1] F. Liu, Y. Yang, Z. Ding, X. Chen, and R. M. Kannel, "Eliminating cross interference between multiple receivers to achieve targeted power distribution for a multi-frequency multi-load MCR WPT system," *IET Power Electron.*, vol. 11, no. 8, pp. 1321–1328, July 2018.

[2] L. Jiang and D. Costinett, "A high-efficiency GaN-based single-stage 6.78 MHz transmitter for wireless power transfer applications," *IEEE Trans. Power Electron.*, vol. 34, no. 8, pp. 7677–7692, Aug. 2019.

[3] K. Lee, C. Jeong, and S. H. Chae, "Analysis of factors effecting on optimal configuration of two receivers for a three-coil wireless power transfer system," *IEEE Syst. J.*, vol. 13, no. 2, pp. 1328–1331, June 2019.

[4] M. Fu, T. Zhang, X. Zhu, P. C.-K. Luk, and C. Ma, "Compensation of cross coupling in multiple-receiver wireless power transfer systems," *IEEE Trans. Ind. Informat.*, vol. 12, no. 2, pp. 474–482, Apr. 2016.

[5] C. Zhong, B. Luo, F. Ning, and W. Liu, "Reactance compensation method to eliminate cross coupling for two-receiver wireless power transfer system," *IEICE Electron. Express*, vol. 12, no. 7, pp. 1–10, Apr. 2015.

[6] Z. Pantic, K. Lee, and S. M. Lukic, "Receivers for multifrequency wireless power transfer: design for minimum interference," *IEEE J. Sel. Topics Power Electron.*, vol. 3, no. 1, pp. 234–241, Mar. 2015.

[7] U. Pratik, B. J. Varghese, A. Azad, and Z. Pantic, "Optimum design of decoupled concentric coils for operation in double-receiver wireless power transfer systems," *IEEE J. Emerg. Sel. Topics Power Electron.*, vol. 7, no. 3, pp. 1982–1998, Sept. 2019.

[8] J. Kuang, B. Luo, Y. Zhang, Y. Hu, and Y. Wu, "Load-isolation wireless power transfer with K-inverter for multiple-receiver applications," *IEEE Access*, vol. 6, pp. 31996–32004, 2018.

[9] J. Zhou, B. Luo, X. Zhang, and Y. Hu, "Extendible load-isolation wireless charging platform for multi-receiver applications," *IET Power Electron.*, vol. 10, no. 1, pp. 134–142, Jan. 2017.

[10] R. Narayanamoorthi, A. V. Juliet, B. Chokkalingam, "Cross interference minimization and simultaneous wireless power transfer to multiple frequency loads using frequency bifurcation approach," *IEEE Trans. Power Electron.*, vol. 34, no. 11, pp. 10898–10909, Nov. 2019.

[11] M. Ishihara, K. Fujiki, K. Umetani, and E. Hiraki, "Automatic active compensation method of cross-coupling in multiple-receiver resonant inductive coupling wireless power transfer systems," in *Proc. IEEE Energy Convers. Congr. Expo.*, Baltimore, MD, USA, 2019, pp. 4584–4591.

[12] S. Seo, H. Jo, and F. Bien, "Free arrangement wireless power transfer system with a ferrite transmission medium and geometry-based performance improvement," *IEEE Trans. Power Electron.*, vol. 35, no. 5, pp. 4518–4532, May 2020.

[13] H. H. Lee, S. H. Kang, and C. W. Jung, "3D-spatial efficiency optimisation of MR-WPT using a reconfigurable resonator-array for laptop applications," *IET Microw. Antennas Propag.*, vol. 11, no. 11, pp. 1594–1602, Sept. 2017.

[14] X. Chen, S. Yu, and Z. Zhang, "A receiver-controlled coupler for multiple output wireless power transfer applications," *IEEE Trans. Circuits Syst. I, Reg. Papers*, vol. 66, no. 11, pp. 4542–4552, Nov. 2019.

[15] M. Ishihara, K. Umetani, and E. Hiraki, "Strategy of topology selection based on quasi-duality between series–series and series–parallel topologies of resonant inductive coupling wireless power transfer systems," *IEEE Trans. Power Electron.*, vol. 35, no. 7, pp. 6785–6798, July 2020.

[16] K. Umetani, T. Honjo, T. Koyama, M. Ishihara, and E. Hiraki, "Receiving-coil structure reducing stray AC resistance for resonant coupling wireless power transfer," *IET. Power Electron.*, vol. 12, no. 9, pp. 2338–2344, Aug. 2019.

[17] S. R. Cove, M. Ordonez, N. Shafiei and J. Zhu, "Improving wireless power transfer efficiency using hollow windings with track-width-ratio," *IEEE Trans. Power Electron.*, vol. 31, no. 9, pp. 6524–6533, Sept. 2016.

[18] Y. Endo, and Y. Furukawa, "Proposal for a new resonance adjustment method in magnetically coupled resonance type wireless power transmission," in *Proc. Int. Microw. Workshop Series on Innovative Wireless Power Transmission: Tech., Syst., and Appl.*, Kyoto, Japan, 2012, pp. 263–266.

[19] A. Kamineni, G. A. Covic, and J. T. Boys, "Self-tuning power supply for inductive charging," *IEEE Trans. Power Electron.*, vol. 32, no. 5, pp. 3467–3479, May 2017.

[20] L. Shi, P. Alou, J. A. Oliver, and J. A. Cobos, "A novel self-adaptive wireless power transfer system to cancel the reactance of the series resonant tank and deliver more power," in *Proc. IEEE Energy Convers. Congr. Expo.*, Baltimore, MD, USA, 2019, pp. 4207–4211.

[21] J.-U. W. Hsu, A. P. Hu, and A. Swain, "A wireless power pickup based on directional tuning control of magnetic amplifier," *IEEE Trans. Ind. Electron.*, vol. 56, no. 7, pp. 2771–2781, July 2009.

[22] R. Mai, Y. Liu, Y. Li, P. Yue, G. Cao, and Z. He, "An active-rectifier-based maximum efficiency tracking method using an additional measurement coil for wireless power transfer," *IEEE Trans. Power Electron.*, vol. 33, no. 1, pp. 716–728, Jan. 2018.

[23] A. Berger, M. Agostinelli, S. Vesti, J. A. Oliver, J. A. Cobos, and M. Huemer, "A wireless charging system applying phase-shift and amplitude control to maximize efficiency and extractable power," *IEEE Trans. Power Electron.*, vol. 30, no. 11, pp. 6338–6348, Nov. 2015.

[24] K. Colak, E. Asa, M. Bojarski, D. Czarkowski, and O. C. Onar, "A novel phase-shift control of semibridgeless active rectifier for wireless power transfer," *IEEE Trans. Power Electron.*, vol. 30, no. 11, pp. 6288–6297, Nov. 2015.

[25] Y. H. Sohn, B. H. Choi, E. S. Lee, G. C. Lim, G.-H. Cho, and C. T. Rim, "General unified analyses of two-capacitor inductive power transfer systems: equivalence of current-source SS and SP compensations," *IEEE Trans. Power Electron.*, vol. 30, no. 11, pp. 6030–6045, Nov. 2015.

[26] S. Huh and D. Ahn, "Two-transmitter wireless power transfer with optimal activation and current selection of transmitters," *IEEE Trans. Power Electron*, vol. 33, no. 6, pp. 4957–4967, June 2018.

[27] E. Ozalevli, N. Femia, G. D. Capua, R. Subramonian, D. Du, J. Sankman, and M. E. Markhi, "A cost-effective adaptive rectifier for low power loosely coupled wireless power transfer systems," *IEEE Trans. Circuits Syst. I, Reg. Papers*, vol. 65, no. 7, pp. 2318–2329, Dec. 2017.

[28] A. Konishi, K. Fujiki, K. Umetani, and E. Hiraki, "Resonant frequency tuning system for repeater resonator of resonant inductive coupling

wireless power transfer," in *Proc. Eur. Conf. Power Electron. Appl.*, Genova, Italy, 2019, pp. 1–10.
[29] M. Ishihara, K. Umetani, and E. Hiraki, "Impedance matching to maximize induced current in repeater of resonant inductive coupling wireless power transfer systems," in *Proc. IEEE Energy Convers. Congr. Expo.*, Portland, OR, USA, 2018, pp. 6194–6201.
[30] D. J. Thrimawithana, U. K. Madawala, and M. Neath, "A synchronization technique for bidirectional IPT systems," *IEEE Trans. Ind. Electron.*, vol. 60, no. 1, pp. 301–309, Jan. 2013.
[31] Y. Lim, H. Tang, S. Lim, and J. Park, "An adaptive impedance-matching network based on a novel capacitor matrix for wireless power transfer," *IEEE Trans. Ind. Electron.*, vol. 29, no. 8, pp. 4403–4413, Aug. 2014.
[32] J. Tian and A. P. Hu, "A DC-voltage-controlled variable capacitor for stabilizing the ZVS frequency of a resonant converter for wireless power transfer," *IEEE Trans. Power Electron.*, vol. 32, no. 3, pp. 2312–2318, Mar. 2017.
[33] J. Osawa, T. Isobe, and H. Tadano, "Efficiency improvement of high frequency inverter for wireless power transfer system using a series reactive power compensator," *in Proc. IEEE Power Electron. Drive Syst. Conf. (PEDS2017)*, Honolulu, HI, USA, 2017, pp. 992–998.
[34] A. Trigui, S. Hached, F. Mounaim, A. C. Ammari, and M. Sawan, "Inductive power transfer system with self-calibrated primary resonant frequency," *IEEE Trans. Power Electron.*, vol. 30, no. 11, pp. 6078–6087, Nov. 2015.
[35] S. Aldhaher, P. C.-K. Luk, and J. F. Whidborne, "Electronic tuning of misaligned coils in wireless power transfer systems," *IEEE Trans. Power Electron.*, vol. 29, no. 11, pp. 5975–5982, Nov. 2014.

**Masataka Ishihara** (Member, IEEE) received the B.S. and M.S. degrees in electrical engineering from Shimane University, Matsue, Japan, in 2015 and 2017, respectively, and Ph.D. degree in electrical engineering from Okayama University, Okayama Japan, in 2021.

He is currently an Assistant Professor with the Okayama University, Okayama, Japan. His research interests include wireless power transfer systems, design of integrated magnetic components, and wide bandgap (WBG) power semiconductor device modeling and driving.

Dr. Ishihara is a Member of the Institute of Electrical Engineers of Japan and the Japan Institute of Power Electronics.

**Keita Fujiki** (Member, IEEE) received the B.S. and M.S. degrees in electrical engineering from Okayama University, Okayama, Japan, in 2018 and 2020, respectively.

He is currently an Engineer with the Toshiba Mitsubishi-Electric Industrial Systems Corporation, Kobe, Japan. His research interest includes wireless power transfer systems.

**Kazuhiro Umetani** (Member, IEEE) received the M.S. and Ph.D. degrees in geophysical fluid dynamics from Kyoto University, Kyoto, Japan, in 2004 and 2007, respectively, and the second Ph.D. degree in electrical engineering from Shimane University, Matsue, Japan, in 2015.

From 2007 to 2008, he was a Circuit Design Engineer with Toshiba Corporation, Japan. From 2008 to 2014, he was with the Power Electronics Group, DENSO Corporation, Japan. From 2014 to 2020, he was an Assistant Professor with the Okayama University, Okayama, Japan. From 2020 to 2021, he was an Associate Professor with the Tohoku University, Miyagi, Japan. He is currently an Associate Professor with the Okayama University, Okayama, Japan. His research interests include new circuit configurations in power electronics and power magnetics for vehicular applications.

Dr. Umetani is a Member of the Institute of Electrical Engineers of Japan and the Japan Institute of Power Electronics.

**Eiji Hiraki** (Member, IEEE) received the M.Sc. and Ph.D. degrees in electrical engineering from Osaka University, Osaka, Japan, in 1990 and 2004, respectively.

He joined Mazda Motor Corporation, Hiroshima, Japan, in 1990. From 1995 to 2013, he was with the Power Electronics Laboratory, Yamaguchi University, Yamaguchi, Japan. He is currently a Professor with the Okayama University, Okayama, Japan. His research interests include circuits and control systems of power electronics, particularly soft-switching technique for high-frequency switching power conversion systems.

Dr. Hiraki is a Member of the Institute of Electrical Engineers of Japan and the Japan Institute of Power Electronics.